

This is the accepted manuscript made available via CHORUS. The article has been published as:

## Active Peltier Coolers Based on Correlated and Magnon- Drag Metals

M.J. Adams, M. Verosky, M. Zebarjadi, and J.P. Heremans

Phys. Rev. Applied **11**, 054008 — Published 3 May 2019

DOI: [10.1103/PhysRevApplied.11.054008](https://doi.org/10.1103/PhysRevApplied.11.054008)

## Active Peltier Coolers based on Correlated and Magnon-drag Metals

M. J. Adams, M. Verosky,  
Department of Mechanical and Aerospace Engineering, The Ohio State University,  
Scott Laboratory, 201 W 19<sup>th</sup> Avenue, Columbus, Ohio 43210, USA

M. Zebarjadi\*  
School of Engineering, University of Virginia  
Thornton Hall, P.O. Box 400259, Charlottesville, VA 22904-4259, USA  
E-mail: [m.zebarjadi@virginia.edu](mailto:m.zebarjadi@virginia.edu)

J. P. Heremans\*  
Department of Mechanical and Aerospace Engineering,  
Department of Physics  
Department of Materials Science and Engineering,  
The Ohio State University,  
Scott Laboratory, 201 W 19<sup>th</sup> Avenue, Columbus, Ohio 43210, USA  
E-mail: heremans.1@osu.edu

Keywords: cooling, active, thermal, Peltier

### Abstract

Active cooling systems use electrical work to bring a hot device (such as an integrated circuit) down to near ambient temperature by draining heat from the hot area of the device to a passive heat sink. Commercial thermoelectric modules are optimized for refrigeration, and are not ideal for active cooling. Refrigeration maintains a temperature that is below the ambient temperature in a device (such as a kitchen refrigerator) by pumping heat from the cold area of the device to a heat sink. The thermoelectric figure of merit  $zT$  is used traditionally to evaluate the performance of thermoelectric modules, including refrigeration modules. But, it is not a good indicator of the performance of active cooling materials. Here, we describe an efficient, all-solid-state active cooler based on the Peltier effect in metals with high thermoelectric power factor due to electron correlation effects (CePd<sub>3</sub>) or magnon drag (Co) and high passive thermal conductivity. We show theoretically and experimentally that the effective thermal conductance under applied current can exceed the limits imposed by Fourier's heat conduction law. The designed device measures an effective thermal

conductance that is an order of magnitude larger than the passive thermal conductance at  $\Delta T=1$  K with the dynamic response of 4 seconds.

## Introduction

As batteries, lasers, high-power electronics, computer chips, and spacecrafts evolve toward more compact structures with high power densities, they require more sophisticated thermal management technology. For example, lithium-ion batteries require careful temperature control, since variations in temperature affect their performance and life-cycle<sup>1</sup>. Similarly, heat management is the limiting step in the further miniaturization of integrated circuits, many of which have time-dependent heat loads.<sup>2-4</sup>

Solid-state compact coolers without moving parts are of high interest in thermal management<sup>5-7</sup>. They are particularly suitable to cooling problems where the thermal load is transient. In such problems, it is useful to have a passive heat sink to handle the steady-state operation, supplemented by an active cooling system that handles peak loads (e.g. during battery charging). Thus, passive and active components typically are combined and both must be optimized simultaneously. An active cooling system (see **figure 1 (a)**) uses electrical work to dissipate heat from the hot area in a device that must be cooled to ambient temperature (e.g., a battery or an electronic circuit), to a reservoir at or near ambient temperature that acts as passive heat sink. The purpose of active cooling is to maximize the heat drained from the hot reservoir while minimizing the temperature drop,  $\Delta T$ , across the cooler. In an all solid-state device, this amounts to maximizing the *effective thermal conductance* of the active cooling system, defined as the ratio of the heat flow out of the hot reservoir to  $\Delta T$ . Normalizing this conductance for geometry, as one does in classical heat transfer problems through passive thermal conductors, one can define an *effective thermal conductivity*  $\kappa_{eff}$  for the materials in such an active cooler:  $\kappa_{eff}$  is the ratio of the heat flux they can carry in active mode to the temperature gradient. For clarity, we note that  $\kappa_{eff}$  is not an intrinsic materials property. Indeed, we will show that  $\kappa_{eff}$  depends on  $\Delta T$  as well as on the intrinsic materials properties  $\kappa$  and the thermoelectric power factor  $PF = \sigma\alpha^2$ , where  $\sigma$  is the electrical conductivity and  $\alpha$  the

thermoelectric power of the material under consideration. Here, we reserve the words *thermal conductivity*  $\kappa$  or *passive thermal conductivity* for the passive heat flux in Fourier's law.

This article describes an all-solid-state approach to achieve this, based on the Peltier effect in metals with high thermopower due to electron correlation effects (CePd<sub>3</sub>) or magnon drag (Co). We show the effective thermal conductance can exceed the limits imposed by Fourier's heat conduction law. We also show how this approach is fundamentally different from Peltier cooling based on conventional thermoelectric (TE) materials such as the (Bi,Sb)<sub>2</sub>(Te,Se)<sub>3</sub> alloys used in commercial Peltier modules.

A TE module has three modes of operations: (1) power generation mode where heat is supplied and electric work is generated; (2) refrigeration mode (**figure 1 (a)**) where electric work is used to pump heat from the area of the device to be maintained below ambient temperatures to a heat sink at or near ambient temperature; and (3) active cooling mode (**figure 1 (a)**) where electric work is used to drain heat from the area of the device to be maintained at or near ambient temperature to a passive heat sink at or near ambient temperature. Commercial Peltier modules are designed for refrigeration applications, including climate controlled automotive seats and small-scale refrigeration of various sensors, or to reduce noise and improve performance of electronic and optoelectronic devices.<sup>6,8,9</sup> For the first two modes of operations, materials with large TE figure of merit,  $zT$ , are needed; in particular, materials with low thermal conductivity. In the power generation mode, low thermal conductivity is needed to maintain the temperature difference. In the refrigeration mode, the idea is to pump heat from cold to hot using electrons. A low lattice thermal conductivity is needed to block the back flux of heat via phonons from hot to cold.

However, for active cooling, material design is different. Traditional high- $zT$  materials are not useful, and instead materials with a simultaneously large TE power factor and passive thermal conductivity are needed to remove heat from a hot area of the device quickly and effectively. Previous studies have already shown that while conventional Peltier TE modules

are able to drive a large heat flux,<sup>10</sup> their effective thermal conductivity in active mode is too small to compete even with the thermal conductivity of metals used in passive heat exchangers.<sup>11</sup> Thus, classical Peltier modules are most useful only in refrigeration mode where the device must be cooled below the ambient temperature, and thus, the temperature of the passive heat sink. In this study, we first point out the differences between the equations that govern active cooling and those that govern refrigeration. Then, we show how these equations lead to different material selection criteria. Finally, we study TE metals experimentally to investigate how to exceed the thermal conductivity of metals in passive heat sinks.

### Theory:

Consider a thermocouple made out of a p- and an n-leg, placed between a hot source and a cold sink. Assume temperature independent materials properties,  $\alpha_{p/n}$ ,  $\sigma_{p/n}$ , and  $\kappa_{p/n}$  to be the Seebeck coefficient, the electrical conductivity, and the thermal conductivity of each leg. Ignoring the contact resistances, the thermal conductance of the TE couple is  $K = \frac{\kappa_p A_p}{L_p} + \frac{\kappa_n A_n}{L_n}$ , the electrical resistance is  $R = \frac{L_p}{\sigma_p A_p} + \frac{L_n}{\sigma_n A_n}$ , and the Seebeck coefficient of the TE couple is  $\alpha = \alpha_p - \alpha_n$ .

In the passive state, shown in **figure 1 (b)**, the rate of heat conduction at the hot side as well as at the cold side of the thermocouple is given by the Fourier's law as:

$$Q_{off} = K(T_H - T_C) \quad (1)$$

where  $T_H$  is the hot source temperature, and  $T_C$  is the cold sink temperature.

The device is switched on by driving an electric current,  $I$ , through the legs, as shown in **figure 1 (c-d)**. Here, there are two possibilities. **Figure 1 (c)** is the refrigeration cycle where heat is pumped from cold side to hot side. In this case, the heat rate extracted from the cold side is

$$Q_{on-refrigeration} = \alpha T_C I - K(T_H - T_C) - RI^2/2 \quad (2)$$

The coefficient of performance (COP) of the refrigerator (a measure of its efficiency) and the maximum temperature drop,  $\Delta T_m$ , it is able to deliver are both limited by the quality of its materials, described by the dimensionless TE figure of merit,  $zT$  of each leg:

$$zT = \frac{\sigma \alpha^2}{\kappa} T \quad (3)$$

Equation (3) demonstrates that  $zT$  benefits from minimizing  $\kappa$ ; thus, a small  $\kappa$  is beneficial to a refrigerator. Commercially available Peltier modules are made from tetradymite materials<sup>12</sup>, which have a thermal conductivity  $\kappa \sim 1 \text{ Wm}^{-1}\text{K}^{-1}$ , a power factor  $PF = \sigma \alpha^2 \sim 33 \text{ } \mu\text{Wcm}^{-1}\text{K}^{-2}$  and material  $zT \sim 1$ .

In the case of active cooling (**figure 1 (d)**), the aim is to increase the rate of heat dissipation from a hot source, adding to Fourier heat conduction. The rate of heat conduction at the hot side is then equal to the sum of Fourier heat conduction and Peltier heat, minus a contribution from Joule heating. Assuming constant temperature boundary conditions, half of the generated Joule heat returns to each end of the leg.<sup>13</sup>

$$Q_{on-active \text{ cooling}} = K(T_H - T_C) + \alpha T_H I - RI^2/2 \quad (4)$$

Taking the derivative, an optimal switching current and maximum rate of heat dissipation are determined:

$$I_{s,optimal} = \alpha T_H / R \quad (5)$$

$$Q_{on-max} = K(T_H - T_C) + (\alpha T_H)^2 / 2R = \left( K + \frac{(\alpha T_H)^2}{2R\Delta T} \right) \Delta T \quad (6).$$

In order to achieve the maximum rate of heat dissipation, TE legs should be chosen with high thermal conductance, large Seebeck coefficient, and low resistance. Optimizing these three parameters is in opposition to the idea that  $zT$  must be maximized.

By analogy with Fourier's law for passive conduction, one can define the term in parenthesis in Equation (6) as the maximum effective thermal conductance. Equation (6) applies to a TE thermocouple, but it could be extended to a single TE leg by writing the

equation in the form of heat flux ( $q''$  in units of  $W/m^2$ ) so that geometrical dependences are removed

$$q''_{on-max} = \left( \kappa + \frac{PF T_H^2}{2 \Delta T} \right) \nabla T \quad (7).$$

$$\kappa_{eff} = \left( \kappa + \frac{PF T_H^2}{2 \Delta T} \right) \quad (8).$$

$\kappa_{eff}$  is the sum of the passive thermal conductivity  $\kappa$  and active thermal conductivity,  $\kappa_{ac} = \frac{PF T_H^2}{2 \Delta T}$ . It is clear that the active term is large when the hot-side temperature is high and the temperature difference is small.

Equation (8) shows that the materials that maximize  $\kappa_{eff}$  have a large  $\kappa$  and a large power factor. Choosing a material with large  $\kappa$  is most important for the passive cooling operating mode. The material property that maximizes  $\kappa_{ac}$ , which determines the performance of the material during active cooling, is the  $PF$ . Materials with simultaneously a large  $\kappa$  and  $\sigma$  are metals, and their  $PF$  is large when their thermopower is. Such metals come in essentially two classes: metals with Kondo effects<sup>14</sup> or correlated electron effects (e.g. CePd<sub>3</sub>),<sup>15</sup> and metals in which the thermopower is dominated by magnon drag (e.g, Co)<sup>16</sup>. In both systems, the Kondo or magnon-drag thermopower can be 10 times larger than the diffusion thermopower in metals, and result in metals with power factors typically two to three times larger than those of high- $zT$  semiconductors.<sup>17,18</sup>

In active mode the thermoelectric module serves only as a pump and the amount of heat  $Q_C$  that the heat sink at  $T_C$  must reject is comprised of both the heat drained at  $T_H$  and the Joule heat dissipated by the Peltier current. Therefore, the active Peltier cooler described requires a larger heat sink at the cold end than a purely passive cooling system would, unless use can be made of a thermal storage system to handle transient active cooling. One can derive that the ratio of heat that must be rejected at the heat sink in active mode to that in passive mode, at a Peltier current of  $I_{s,optimal}$ , is:



$$\frac{Q_{con}}{Q_{off}} = (1 + \frac{zT_H}{\Delta T} (T_c + \frac{T_H}{2})) \quad (9)$$

## Experiment

To verify the model and the statements made above experimentally, an active cooler was constructed from a Co/CePd<sub>3</sub> TE couple and its performance measured in the configuration 1(d). Cobalt foil was selected for the n-type leg because it has a peak power factor (PF) of 160  $\mu\text{Wcm}^{-1}\text{K}^{-2}$  in the temperature range of 300-400 K, which is about 3-4 times larger than conventional bismuth telluride.<sup>17</sup> Fewer options are available for the choice of high-PF, high- $\kappa$  p-type metals. CePd<sub>3</sub> was selected for its peak PF  $\sim 90 \mu\text{Wcm}^{-1}\text{K}^{-2}$ , though it has a lower thermal conductivity.<sup>15</sup>

The materials were cut into proportions that give the same length of 4.3 mm. The two materials have dissimilar thermopower and resistivity. Therefore, the cross section of the CePd<sub>3</sub> leg is about 3.7 times larger than the Co leg to match their electrical and thermal conductance to each other, as is done with commercial Peltier modules.<sup>18</sup> Each leg was soldered to an alumina base plate, which was attached to a copper heat sink with thermally conductive paste. A resistive heating element was mounted on top with a copper heat spreader. Type T thermocouples of 25  $\mu\text{m}$  diameter and a few cm in length measure temperature difference along the length of the thermocouple; they drain negligible heat out of the Co/CePd<sub>3</sub> thermocouple. Experiments were performed at room temperature in a vacuum chamber with a radiation shield over the sample.

## Results

Combining the data from Watzman<sup>16</sup> with the formula for effective thermal conductivity in Equation (8), Co is modeled to reach  $\kappa_{eff} \sim 1500 \text{ Wm}^{-1}\text{K}^{-1}$  at  $\Delta T = 1 \text{ K}$ , as shown in **figure 2 (a)**. Similarly, using data from Boona,<sup>15</sup> CePd<sub>3</sub> is expected to have a  $\kappa_{eff} \sim 600 \text{ Wm}^{-1}\text{K}^{-1}$  at a  $\Delta T = 1 \text{ K}$ . (see **figure 2 (b)**).

Both metals are combined in one module as explained in the experimental section. First, a refrigeration experiment was performed in the configuration of Fig. 1(c) to determine optimal electric current: the value of  $T_C - T_H$  in refrigeration mode was measured as a function of  $I_S$ . This followed a parabolic relation  $(T_C - T_H)_{\text{Refrigeration}} = -0.14 - 3.04 I_S + 0.28 I_S^2$ , a function that has a minimum for  $I_S = 5.4 \pm 0.6$ ; the value of  $(T_C - T_H)$  varies by less than 1% over that interval, the measurement accuracy of the thermometry. We chose an optimal switching current at the low end of this range to limit the heat load on the heat exchanger:  $I_{S,\text{optimal}} = 5$  amps, which gives a  $\Delta T_{\text{Refrigeration}} = 8.5$  K in the absence of a heat load. Second, thermal conductance was measured by the static heater-and-sink method (configurations Fig. 1 (b) and (d)). A heat load was generated at the top of the thermocouple so that the device sat between a hot source and cold sink. The resulting temperature difference was measured as a function of heater power in both passive (zero  $I_S$ , configuration Fig. 1 (b)) and active (current  $I_{S,\text{optimal}}$ , configuration Fig. 1 (d)) cooling states. **Figure 3 (a)** shows the steady-state measurement of the heat flow  $Q$  for a given temperature drop  $\Delta T$  both in passive mode and in active mode under optimum current. Transient measurements of the  $\Delta T$  versus time are shown in **figure 3 (b)**: an experimental time constant of  $\tau \sim 4$  seconds is determined by normalizing the data and fitting an exponential function.

The measured thermal conductance ( $Q/\Delta T$ ) is converted into an effective thermal conductivity, shown in **figure 4** for various values of  $\Delta T = T_H - T_C$ . The values are compared to theoretical values calculated from the predicted effective thermal conductivity of each material (Eq. 8) and their relative cross-sectional areas:

$$\kappa_{th} = (A_{Co}\kappa_{eff,Co} + A_{CePd3}\kappa_{eff,CePd3})/(A_{Co} + A_{CePd3}) \quad (10).$$

As predicted by theory, the effective thermal conductivity of the cooler can exceed  $1000 \text{ Wm}^{-1}\text{K}^{-1}$  in its active mode versus  $40 \text{ Wm}^{-1}\text{K}^{-1}$  in passive mode. The upper frame of **figure 4** shows the relative deviation between the values calculated from the material

properties and Equation (8), and the measured values. The measured values are within 10% of theoretical values for this temperature range; since thermal contact resistances were ignored in the calculation, the agreement mainly signifies that contact resistances are also much less of a problem with metal TE elements than they are with semiconductor ones. For small values of thermal conductivity, experimental measurements tend to be greater than theoretical values, indicating radiative losses in the experiment. Under the condition of optimal electric current and small temperature difference, thermal conductance is large and radiative losses become negligible. Electrical contact resistances are not quantified, since calculations and experiments consider only currents, but no additional heating is observed that could be ascribed to them.

The time constant measured in **figure 3 (b)** is also calculated using the formula  $\tau = C_{th}/K$ . The device thermal conductance,  $K = 0.008 \text{ W/K}$ , is calculated from the passive thermal conductivity of each element and its dimensions. Combining  $K$  with the calculated thermal capacity of each of the components in the cooling module, a time constant  $\tau$  is estimated to be 3.6 seconds, which is close to the measured value. Thus, the response time is a function only of the passive thermal diffusivity of the materials. Therefore, the response time is expected to be proportional to the square of the length of the TE legs. Furthermore, the high value of  $\kappa$  in metals is beneficial to the transient response of the coolers. Finally, for any particular application, optimum designs can be found that will trade off response time for current and the  $Q/(T_H - T_C)$  ratio.

In summary, the effective thermal conductivity, and thus the cooling capacity, of an active Peltier cooling module constructed from high power factor, high thermal conductivity metals has been demonstrated to exceed the thermal conductivity of materials used in passive heat sinks by up to an order of magnitude, depending on the temperature differences. As predicted by theory, effective thermal conductivity diverges at small temperature differences. A Co/CePd<sub>3</sub> Peltier couple produced a measurable conductivity of over  $1000 \text{ Wm}^{-1}\text{K}^{-1}$  under temperature differences of less than one degree, which is 25 times larger than the passive

thermal conductivity of the couple. Materials for the p-type leg are harder to find than for the n-type leg: new Pd-free p-type metals are needed to lower costs. Metal TEs can have an additional advantage in active cooling because, unlike conventional materials, they can be integrated with existing fin heat exchangers. When TE legs are used as fins, much larger heat fluxes can be extracted.

## Acknowledgements

M.J.A. was supported by the Ford-OSU alliance 2017 program. M.Z. acknowledges support from National Science Foundations, grant number 1653268. The authors acknowledge Steve Boona for preparing the CePd<sub>3</sub> material.

Received: ((will be filled in by the editorial staff))

Revised: ((will be filled in by the editorial staff))

Published online: ((will be filled in by the editorial staff))

## References

- <sup>1</sup> J. Kim, J. Oh, and H. Lee, "Review on Battery Thermal Management System for Electric Vehicles," *Appl. Therm. Eng.* **149**, 192 (2019).
- <sup>2</sup> E. Pop, S. Sinha, and K.E. Goodson, "Heat Generation and Transport in Nanometer-scale Transistors," *Proc. IEEE* **94**, 1587 (2006).
- <sup>3</sup> V. Sahu, A.G. Fedorov, Y. Joshi, K. Yazawa, A. Ziabari, and A. Shakouri, "Energy Efficient Liquid-Thermoelectric Hybrid Cooling for Hot-spot Removal," in *Semicond. Therm. Meas. Manag. Symp. (SEMI-THERM), 2012 28th Annu. IEEE* (2012), pp. 130–134.
- <sup>4</sup> A. Shakouri, "Nanoscale Thermal Transport and Microrefrigerators on a Chip," *Proc. IEEE* **94**, 1613 (2006).
- <sup>5</sup> G. Wehmeyer, T. Yabuki, C. Monachon, J. Wu, and C. Dames, "Thermal Diodes, Regulators, and Switches: Physical Mechanisms and Potential Applications," *Appl. Phys. Rev.* **4**, 041304 (2017).
- <sup>6</sup> A. Ziabari, M. Zebarjadi, D. Vashaee, and A. Shakouri, "Nanoscale Solid-state Cooling: A Review," *Reports Prog. Phys.* **79**, 095901 (2016).
- <sup>7</sup> L.E. Bell, "Cooling, Heating, Generating Power, and Recovering Waste Heat with Thermoelectric Systems," *Science* **321**, 1457 (2008).
- <sup>8</sup> W. Seifert, V. Pluschke, and N.F. Hinsche, "Thermoelectric Cooler Concepts and the Limit for Maximum Cooling," *J. Phys. Condens. Matter* **26**, 255803 (2014).
- <sup>9</sup> G.J. Snyder, E.S. Toberer, R. Khanna, and W. Seifert, "Improved Thermoelectric Cooling

Based on the Thomson Effect," Phys. Rev. B **86**, 045202 (2012).

<sup>10</sup> I. Chowdhury, R. Prasher, K. Lofgreen, G. Chrysler, S. Narasimhan, R. Mahajan, D. Koester, R. Alley, and R. Venkatasubramanian, "On-chip Cooling by Superlattice-based Thin-film Thermoelectrics," Nat. Nanotechnol. **4**, 235 (2009).

<sup>11</sup> M. Zebarjadi, "Electronic Cooling using Thermoelectric Devices," Appl. Phys. Lett. **106**, 203506 (2015).

<sup>12</sup> J.P. Heremans, R.J. Cava, and N. Samarth, "Tetradymites as Thermoelectrics and Topological Insulators," Nat. Rev. Mater. **2**, 17049 (2017).

<sup>13</sup> T.L. Bergman, A.S. Lavine, F.P. Incropera, and D.P. DeWitt, *Introduction to Heat Transfer*, 6th ed. (John Wiley and Sons, Inc., Hoboken, NJ, 2011).

<sup>14</sup> M.K. Fuccillo, Q.D. Gibson, M.N. Ali, L.M. Schoop, and R.J. Cava, "Correlated Evolution of Colossal Thermoelectric Effect and kondo Insulating Behavior," APL Mater. **1**, 062102 (2013).

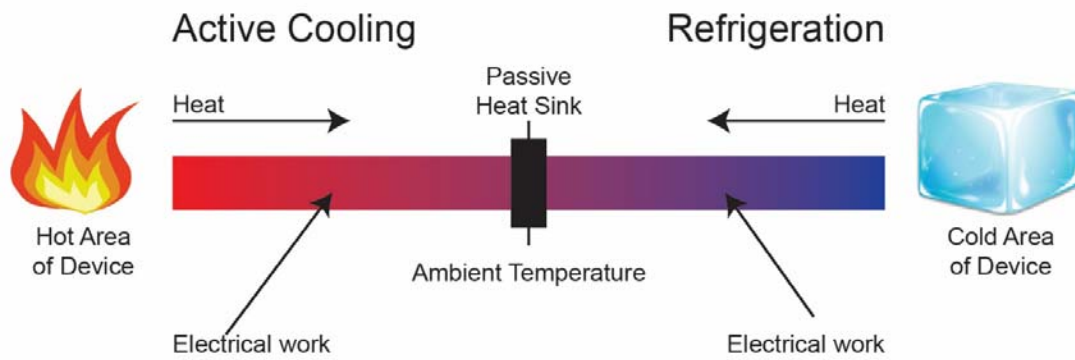
<sup>15</sup> S.R. Boona and D.T. Morelli, "Enhanced Thermoelectric Properties of CePd<sub>3-x</sub>Pt<sub>x</sub>," Appl. Phys. Lett. **101**, 101909 (2012).

<sup>16</sup> S.J. Watzman, R.A. Duine, Y. Tserkovnyak, S.R. Boona, H. Jin, A. Prakash, Y. Zheng, and J.P. Heremans, "Magnon-drag Thermopower and Nernst Coefficient in Fe, Co, and Ni," Phys. Rev. B **94**, 144407 (2016).

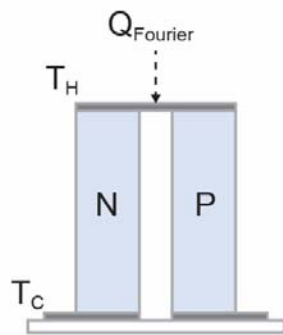
<sup>17</sup> B. Poudel, Q. Hao, Y. Ma, Y. Lan, A. Minnich, B. Yu, X. Yan, D. Wang, A. Muto, D. Vashaee, X. Chen, J. Liu, M.S. Dresselhaus, G. Chen, and Z. Ren, "High Thermoelectric Performance of Nanostructured Bismuth Antimony Telluride Bulk Alloys," Science **320**, 634 (2008).

<sup>18</sup> R.W. Ure, "Theoretical Calculation of Device Performance," in *Thermoelectricity*, (R.R. Heikes and R.W. Ure, Eds., Interscience Publishers, New York, 1961).

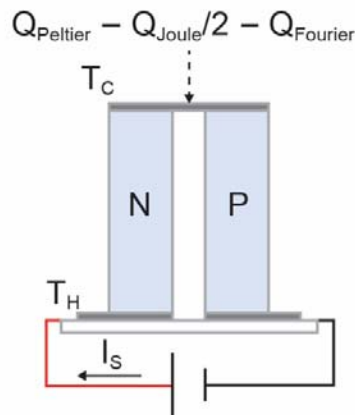
(a)



(b)



(c)



(d)

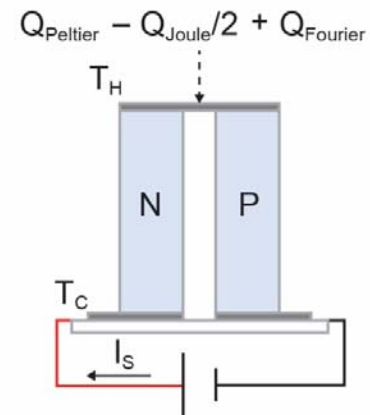


**Figure 1.** Schematic drawings show (a) the difference between active cooling and refrigeration, and (b-d) the use of Peltier couples in various modes of heat conduction: (b) passive mode, (c) refrigeration mode, (d) active cooling mode.

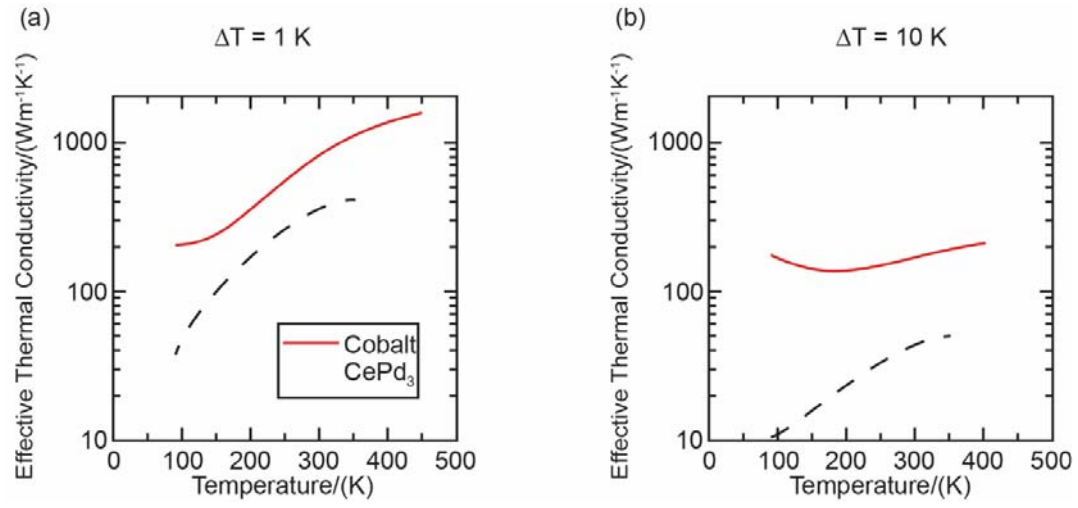


**Figure 2.** Calculated values of effective thermal conductivity. The red lines represent the  $\kappa_{eff}$  of Co and black dashes represent that of CePd<sub>3</sub> (a) for  $\Delta T=1$  K and (b) for  $\Delta T=10$  K



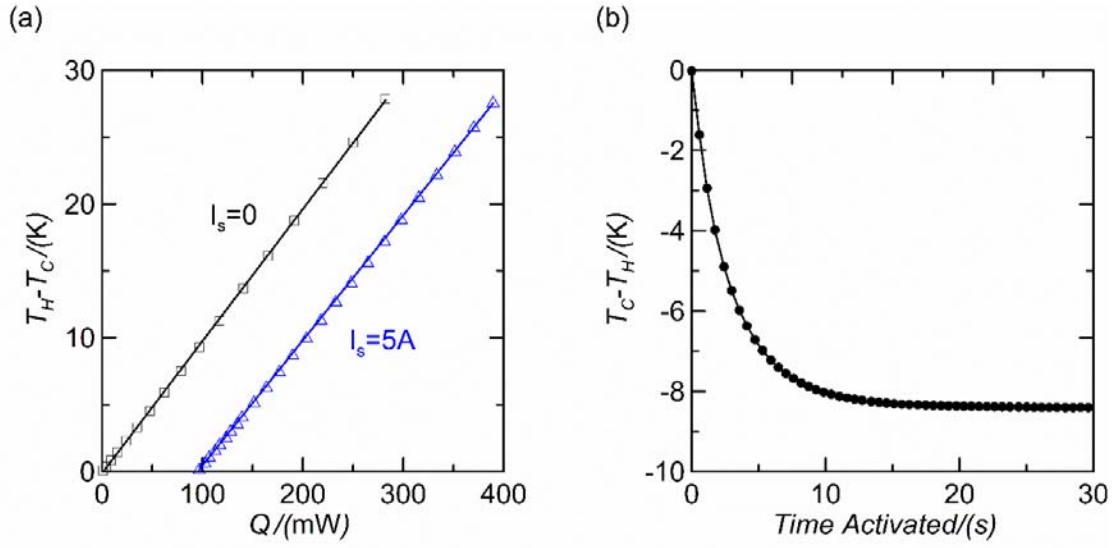


**Figure 3.** Data measured on a Co/CePd<sub>3</sub> TE couple cooler under a Peltier current  $I_s$ . (a) The temperature difference as a function of the heat load; the slope of these lines gives the thermal conductance. (b) The time dependence of the temperature drop after  $I_s$  is switched on.

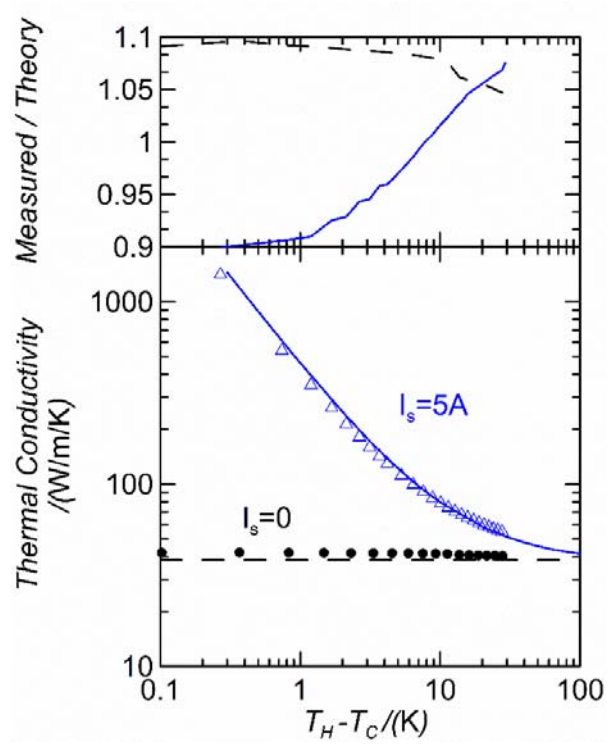


**Figure 4.** Effective thermal conductivity of the Co/CePd<sub>3</sub> TE couple cooler for two values of  $I_s$ . In the bottom frame, the symbols represent measured points and lines represent theory. The top frame (the same colors identify  $I_s$  as in the bottom frame) shows the deviation between theory and experiment to be less than 10% for the same currents as are used in the bottom frame.